Supporting Information for

On the Temperature Dependence of Hydroxymethyl Group Rotamer Populations in Cellooligomers

Thibault Angles d'Ortoli,[†] Nils A. Sjöberg,[‡] Polina Vasiljeva,[‡] Jonas Lindman,[‡] Göran Widmalm,[†] Malin Bergenstråhle-Wohlert,[‡] and Jakob Wohlert[‡]**

†Department of Organic Chemistry, Arrhenius Laboratory, Stockholm University, SE-106 91 Stockholm, Sweden

‡Wallenberg Wood Science Center, and the Department of Fibre and Polymer Technology, KTH Royal Institute of Technology, SE-100 44 Stockholm, Sweden

* Email: goran.widmalm@su.se

* Email: jacke@kth.se

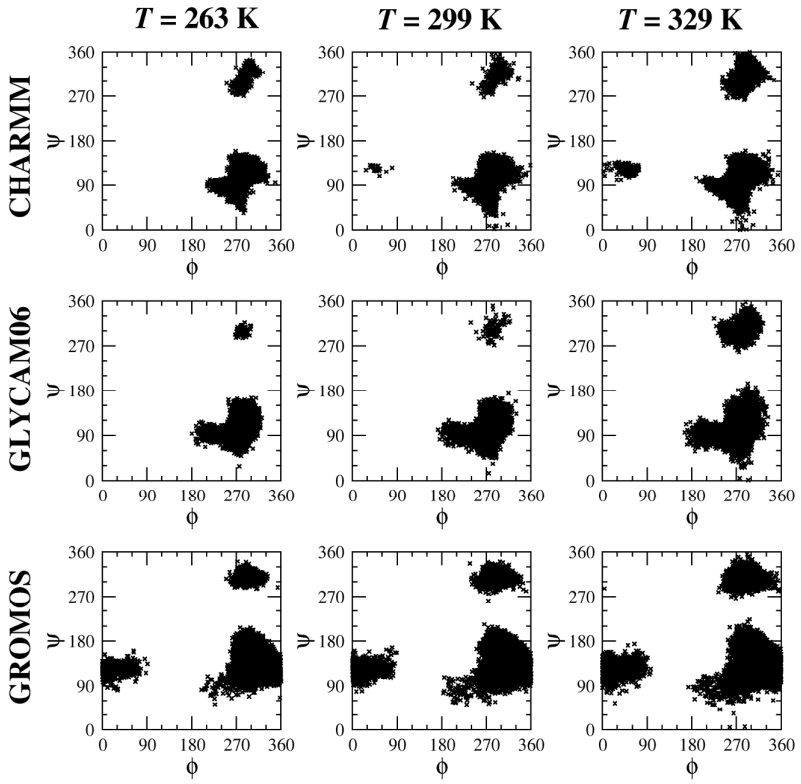

Figure S1. Scatter plots of the two torsion angles ϕ = O5' – C1' – O4 – C4 and ψ = C1' – O4 – C4 – C3 in degrees that define the conformation of the glycosidic linkage in methyl β-cellobioside.

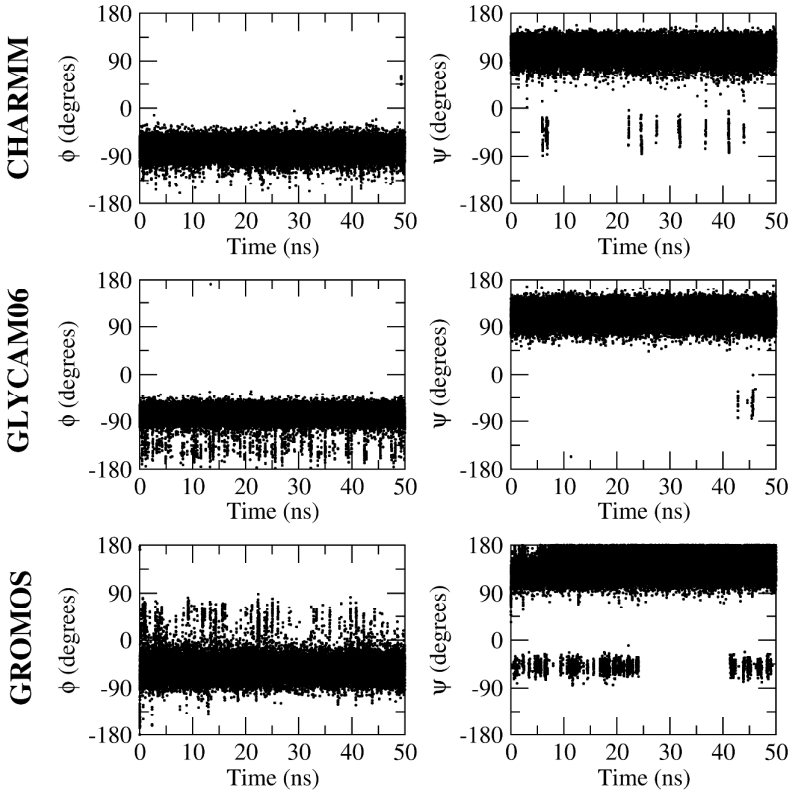

Figure S2. Time evolution of the torsion angles ϕ and ψ of the glycosidic linkage at room temperature.

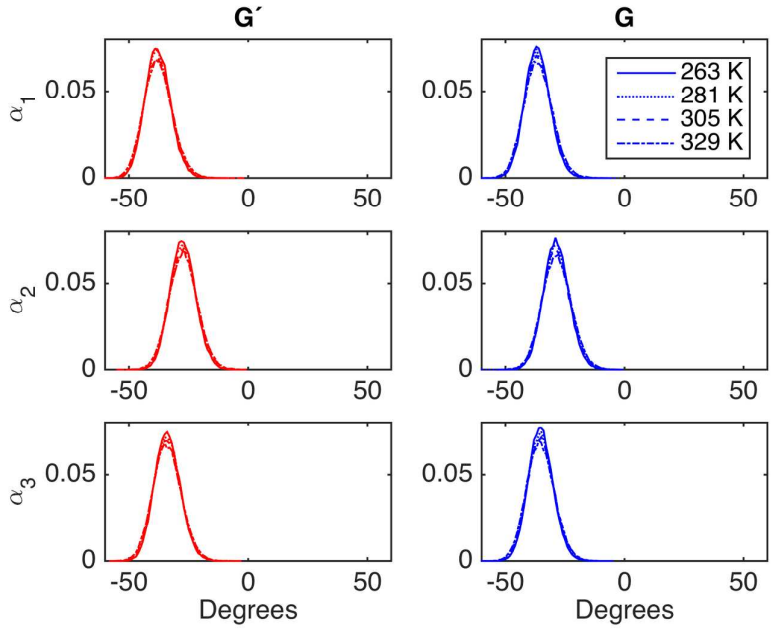

Figure S3. Distributions of the pseudo-dihedral angles α_1, α_2, and α_3 in methyl β-cellobioside using the CHARMM C35 force field, for the non-reducing (G') and reducing (G) ends separately.

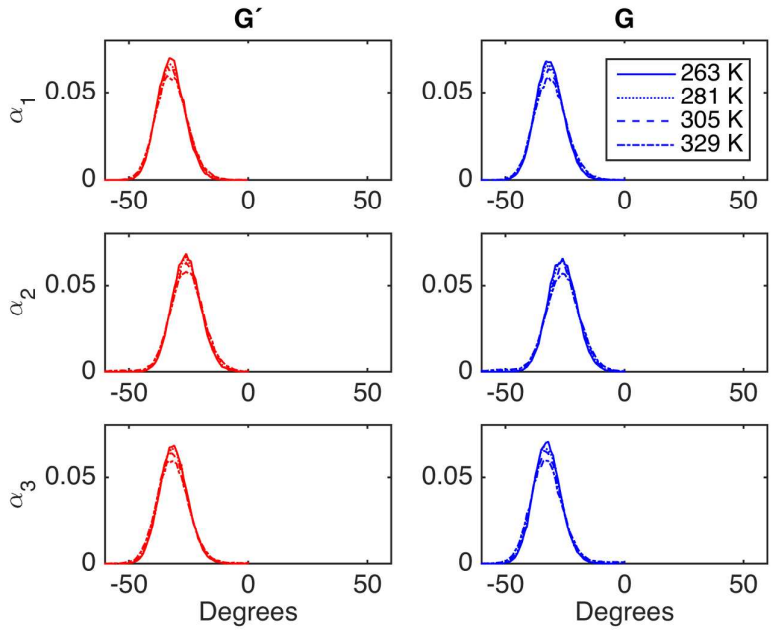

Figure S4. Distributions of the pseudo-dihedral angles α_1, α_2, and α_3 in methyl β-cellobioside using the GLYCAM06 force field, for the non-reducing (G') and reducing (G) ends separately.

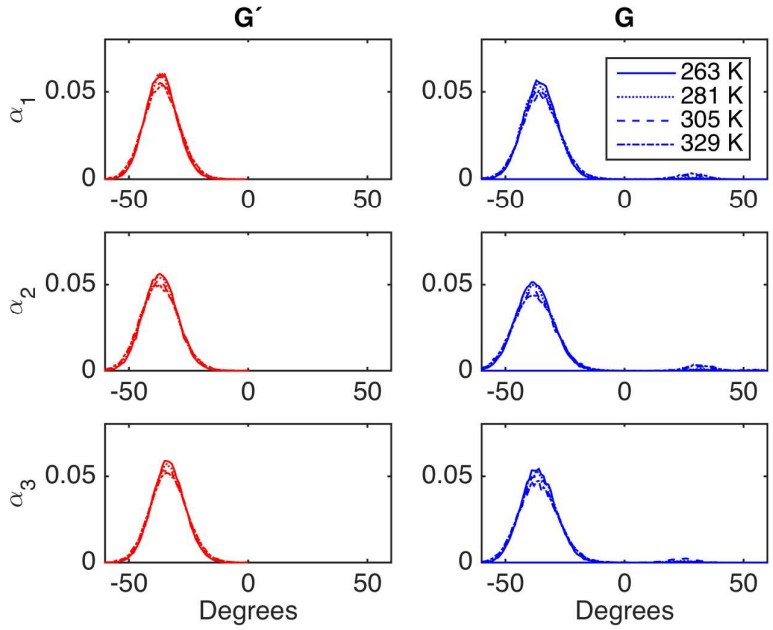

Figure S5. Distributions of the pseudo-dihedral angles α_1, α_2, and α_3 in methyl β-cellobioside using the GROMOS $56A_{carbo}$ force field, for the non-reducing (G') and reducing (G) ends separately.

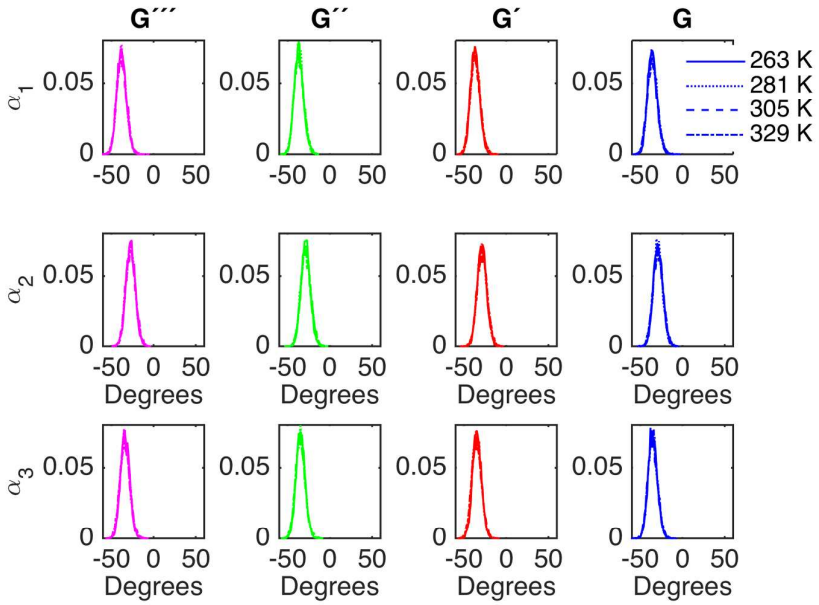

Figure S6. Distributions of the pseudo-dihedral angles α_1, α_2, and α_3 in β-cellotetraose using the CHARMM C35 force field, for the non-reducing end (G‴), the inner segments (G″, G′) and the reducing (G) end separately.

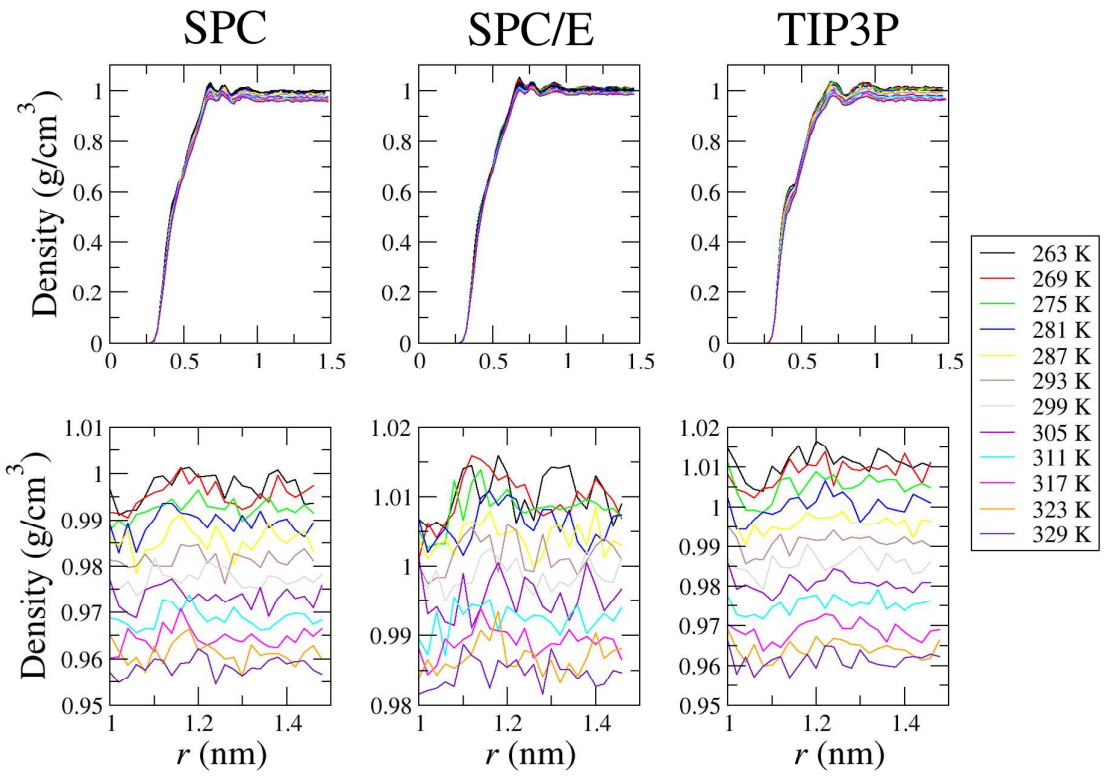

Figure S7. Top: Un-normalized radial distribution functions between the solute and the solvent molecules, showing how the solvent bulk densities vary with temperature. Bottom: Magnifications of the plateau regions.

Table S1. Calculated $^3J_{HH}$ coupling constants in methyl β-cellobioside as a function of temperature using the CHARMM C35 force field.

	$^3J_{HH}$ Terminal End (Hz)		$^3J_{HH}$ Reducing End (Hz)	
T (K)	H5'-H6'$_{pro\text{-}R}$	H5'-H6'$_{pro\text{-}S}$	H5-H6$_{pro\text{-}R}$	H5-H6$_{pro\text{-}S}$
263	5.59	1.81	4.62	1.86
269	5.65	1.85	4.55	1.93
275	5.79	1.93	4.65	2.00
281	5.85	1.97	4.79	2.09
287	6.00	2.02	4.98	2.14
293	6.24	2.06	4.89	2.22
299	6.40	2.12	4.83	2.30
305	6.54	2.21	4.80	2.35
311	6.64	2.22	4.83	2.44
317	6.76	2.26	5.02	2.54
323	6.84	2.32	5.24	2.67
329	6.81	2.43	5.38	2.76

Table S2. Calculated $^3J_{HH}$ coupling constants in methyl β-cellobioside as a function of temperature using the GLYCAM06 force field.

	$^3J_{HH}$ Terminal End (Hz)		$^3J_{HH}$ Reducing End (Hz)	
T (K)	H5'-H6'$_{pro\text{-}R}$	H5'-H6'$_{pro\text{-}S}$	H5-H6$_{pro\text{-}R}$	H5-H6$_{pro\text{-}S}$
263	3.98	1.74	2.61	1.63
269	4.10	1.75	2.72	1.65
275	4.12	1.75	2.79	1.67
281	4.28	1.78	2.91	1.69
287	4.52	1.78	3.18	1.71
293	4.71	1.82	3.42	1.76
299	4.79	1.87	3.62	1.79
305	5.07	1.90	3.82	1.82
311	5.22	1.93	4.12	1.87
317	5.39	1.94	4.52	1.92
323	5.42	1.97	4.71	2.01
329	5.47	2.00	4.89	2.11

Table S3. Calculated $^3J_{HH}$ coupling constants in methyl β-cellobioside as a function of temperature using the GROMOS 56A$_{carbo}$ force field.

	$^3J_{HH}$ Terminal End (Hz)		$^3J_{HH}$ Reducing End (Hz)	
T (K)	H5'-H6'$_{pro\text{-}R}$	H5'-H6'$_{pro\text{-}S}$	H5-H6$_{pro\text{-}R}$	H5-H6$_{pro\text{-}S}$
263	5.60	2.28	4.72	2.14
269	5.58	2.30	4.77	2.14
275	5.60	2.30	4.81	2.19
281	5.67	2.34	4.80	2.23
287	5.64	2.36	4.89	2.27
293	5.64	2.41	4.96	2.33
299	5.60	2.42	5.03	2.38
305	5.65	2.44	5.16	2.44
311	5.66	2.46	5.22	2.47
317	5.77	2.44	5.25	2.50
323	5.74	2.49	5.27	2.52
329	5.76	2.50	5.29	2.56